SUPPLEMENTARY MATERIALS

Title: Th9 cells promote antitumor responses in vivo

Authors: Yong Lu, Sungyoul Hong, Haiyan Li, Jungsun Park, Bangxing Hong, Lijuan Wang, Yuhuan Zheng, Zhiqiang Liu, Jinda Xu, Jin He, Jing Yang, Jianfei Qian, and Qing Yi

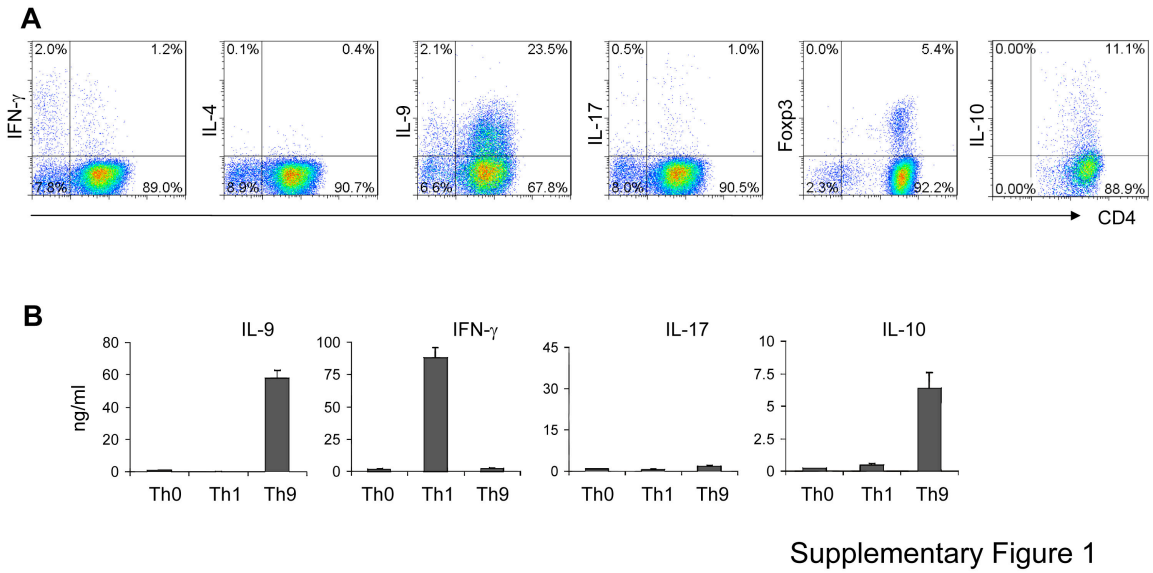

Supplementary Figure 1

Supplementary Figure 1. Cytokine profiles of polarized Th cells. Naive $CD4^+CD62L^+$ T cells were purified from the spleens of OT-II mice, and cocultured with irradiated APCs under polarized conditions detailed in Methods. (**A**) ICS showing the percentages of cytokine-producing or Foxp3-expressing $CD4^+$ cells in polarized Th9 cells. (**B**) ELISA shows the levels of secreted cytokines in the culture supernatants of polarized Th0, Th1, and Th9 cells. Supernatants were collected on day 3 of restimulation, and cytokine levels in the supernatants were measured by ELISA.

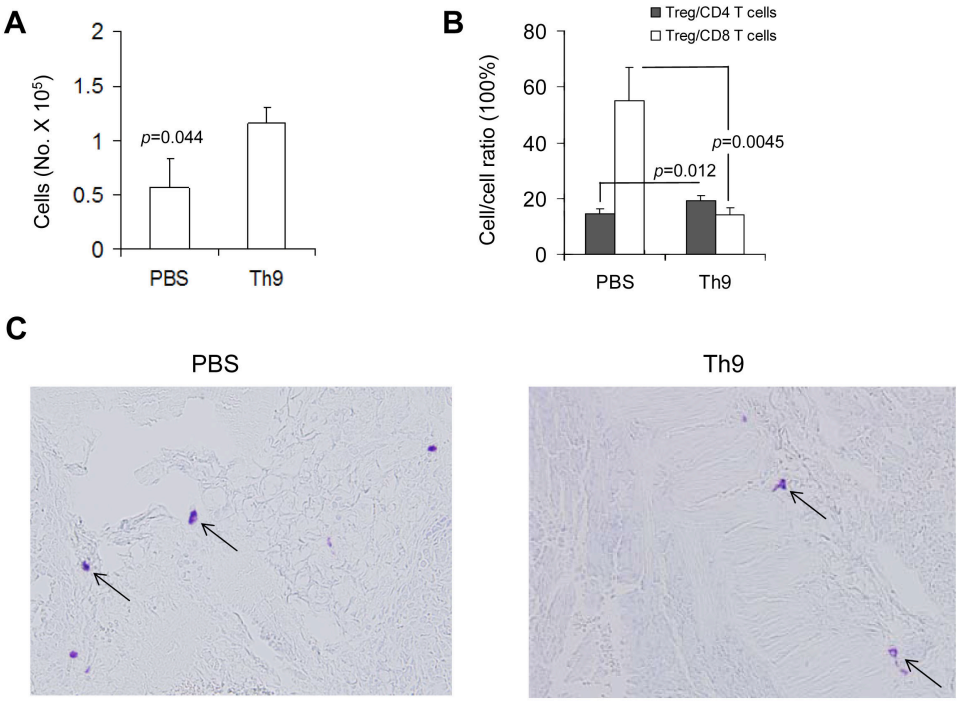

Supplementary Figure 2

Supplementary Figure 2. Analysis of tumor-infiltrating Treg cells and mast cells in PBS and Th9 cell-treated mice. (**A**) FACS analysis of total Treg cell numbers in the lung leukocyte fraction of PBS and Th9 cell-treated tumor-bearing mice from the prevention model. (**B**) Treg cells to total $CD4^+$ T cells or $CD8^+$ T cells ratios were calculated from FACS analysis in the lung leukocyte fraction of PBS and Th9 cell-treated tumor-bearing mice. The *p* values in the graphs show comparison with PBS or as indicated. (**C**) Mast cells were visualized using Toluidine Blue Staining in lung sections of PBS and Th9 cell-treated tumor-bearing mice. Arrows indicate positive staining of mast cells. Note: Although we show some positive staining of mast cells in these two views, mast cells were absent in most of the view fields; About 10 mast cells in each whole lung section were detected, and there was no difference between PBS and Th9 cell-treated mice. Original magnification: ×200.

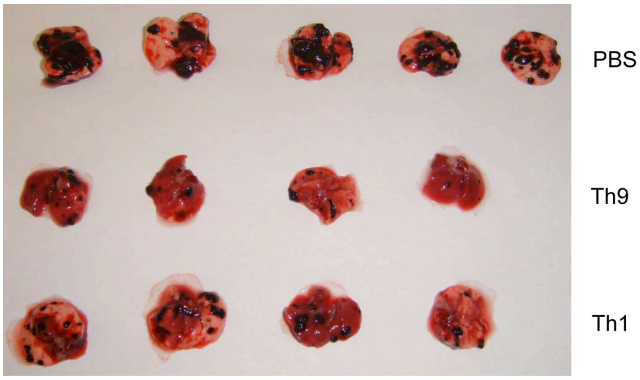

Supplementary Figure 3

Supplementary Figure 3. Images of lung metastasis in Th9-treated mice. PBS or 3 × 10^6 Th1 or Th9 cells were i.v. transferred into C57BL/6 mice bearing 5-day established pulmonary B16-OVA melanoma. Mice (n = 4~5/group) were analyzed on day 19 after challenge. Photos of the lungs of mice receiving different treatments are shown.

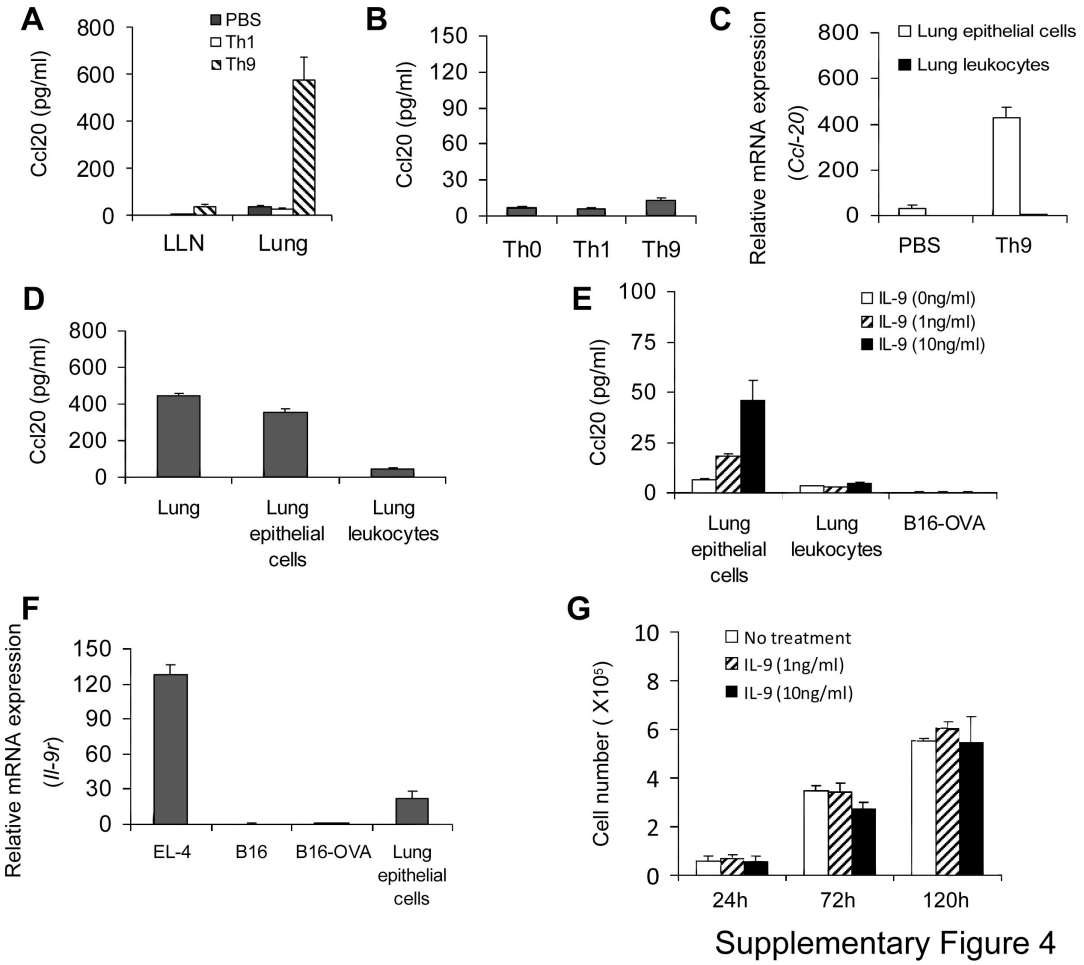

Supplementary Figure 4. Main source of Ccl20 in Th9 cell-treated mice. (**A**) Ccl20 levels in culture supernatants were measured by ELISA. Supernatants were collected from wild-type mice as shown in Figure 4A. (**B**) Ccl20 production in culture supernatants of polarized Th0, Th1, and Th9 cells. (**C**) RT-PCR analysis of *Ccl20* mRNA expression by lung epithelial cells and leukocytes. Data shown were normalized to gene β-*actin*. (**D**) Ccl20 production in culture supernatants of lung epithelial cells and leukocytes isolated from Th9 cell-treated tumor-bearing mice. (**E**) Ccl20 production in culture supernatants of lung epithelial cells, leukocytes and B16-OVA tumor cells in response to IL-9 stimulation. (**F**) RT-PCR analysis of *Il-9r* mRNA expression by lung epithelial cells and tumor cells. Data shown were normalized to gene β-*actin*. EL-4 cells were used as positive control. (**G**) IL-9 was added to B16-OVA tumor cell culture and tumor cell growth was shown by counting tumor cell number.

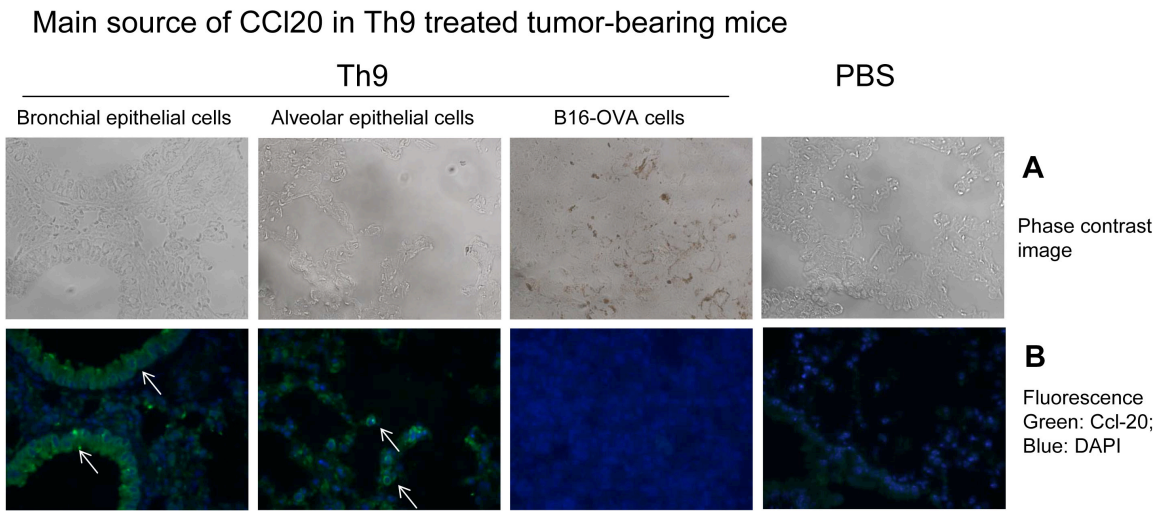

Supplementary Figure 5

Supplementary Figure 5. Immunofluorescence analysis of Ccl20 production in Th9 cell-treated mice. (**A**) Phase contrast images show the morphology of epithelial cells and tumor cells in lung sections of PBS and Th9 cell-treated tumor-bearing mice. (**B**) Immunofluorescence analysis shows the production of Ccl20 (green) by lung epithelial cells in lung sections of Th9 cell-treated tumor-bearing mice. Arrows indicate Ccl20 positive cells. Original magnification: ×400.

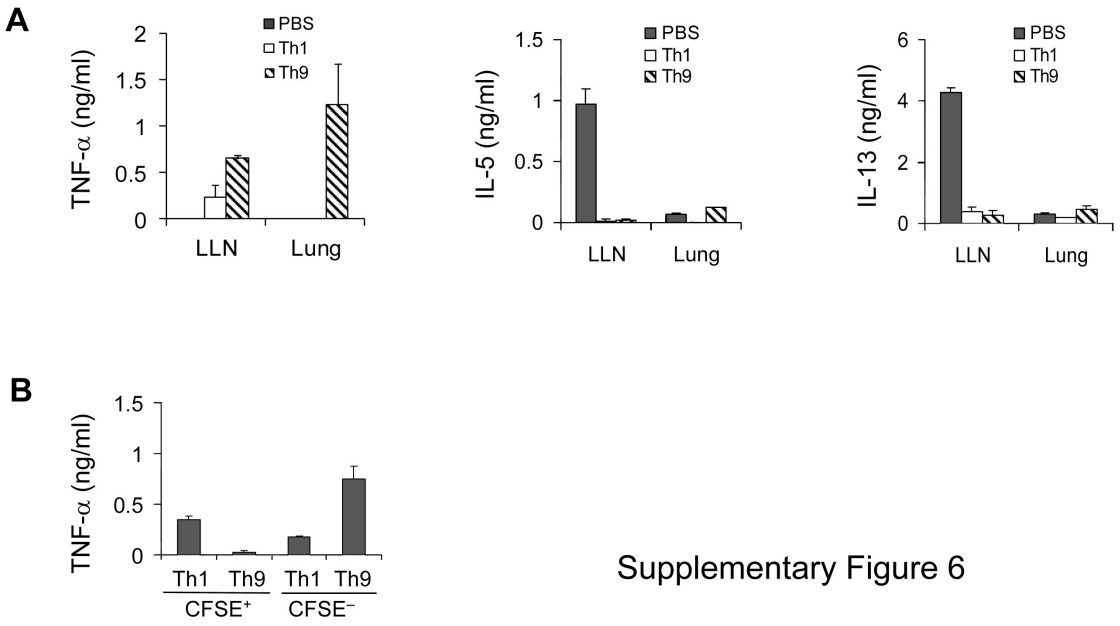

Supplementary Figure 6. Production of TNF-α, IL-5 and IL-13 in Th9 cell-treated mice. (**A**) Cytokine levels in culture supernatants were measured by ELISA. Supernatants were collected from wild-type mice as shown in Figure 4A. (**B**) TNF-α levels in culture supernatants were measured by ELISA. Supernatants were collected as shown in Figure 4B.

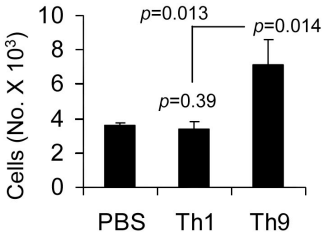

Supplementary Figure 7

Supplementary Figure 7. Infiltration of OT-I CD8$^+$ T cells in the lung. CFSE-labeled OT-I CD8$^+$ T cells (3×10^6) were i.v. transferred into C57BL/6 mice (n = 3/group) that were bearing 5-day pulmonary B16-OVA melanoma and were also iv transferred with 3×10^6 Th1 or Th9 cells. Mice were sacrificed 3 days later, and CFSE$^+$ OT-I cells in lung leukocyte population were enumerated by FACS. The *p* values in the graphs show comparison with PBS or as indicated.

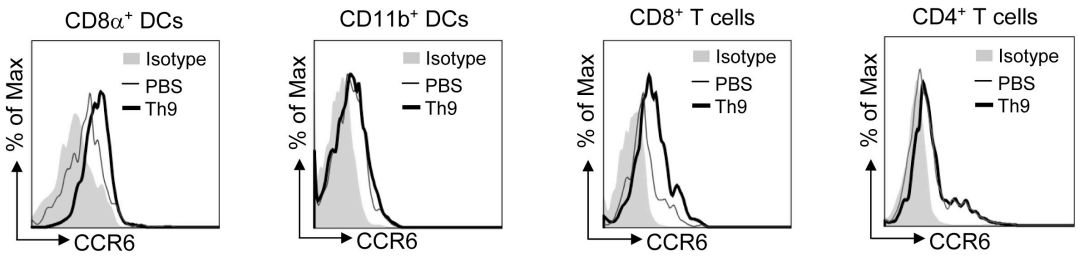

Supplementary Figure 8

Supplementary Figure 8. Surface expression of Ccr6. Mice were sacrificed at the endpoint of experiments shown in Figure 2B. LLN cells were analyzed by FACS for Ccr6 expression by DC populations. Lung tumor tissue-infiltrating $CD8^+$ and $CD4^+$ T cells were also analyzed by FACS for surface Ccr6 expression. Representative histograms of $CD8\alpha^+$ DCs, $CD11b^+$ DCs, $CD8^+$ and $CD4^+$ T cells are shown.

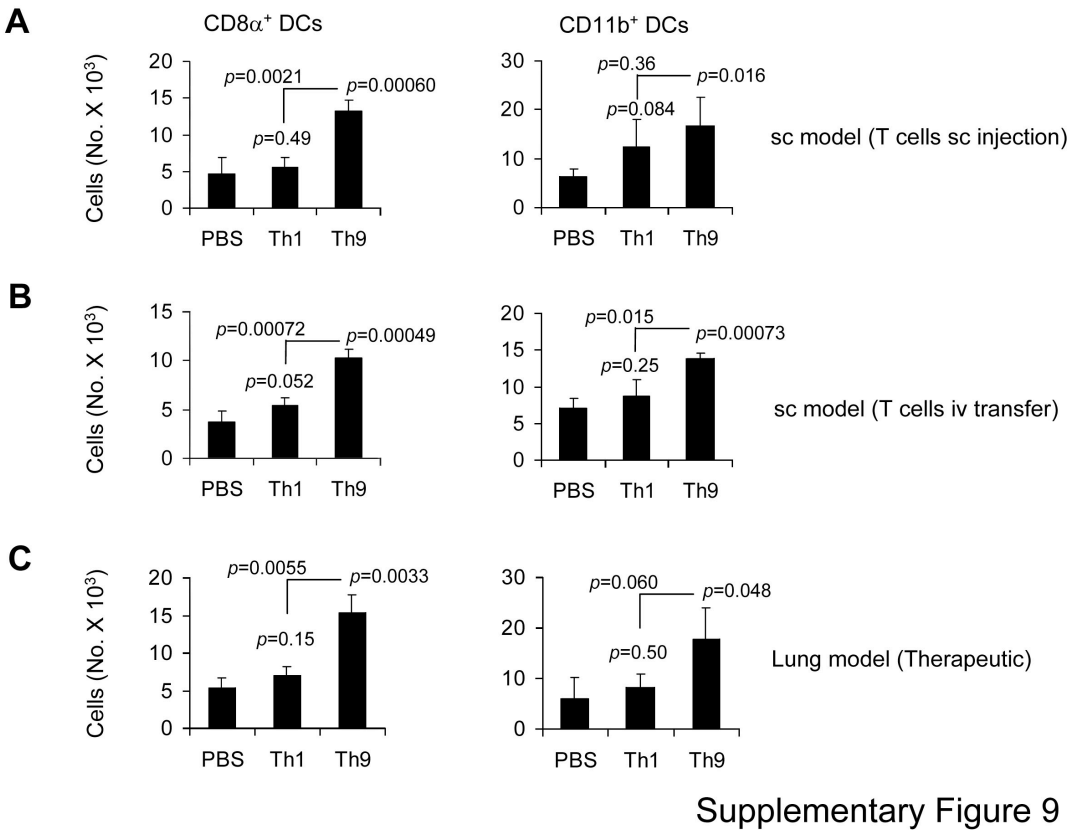

Supplementary Figure 9. Analysis of CD11c$^+$ DCs in the TDLNs. Mice (**A**, **B** and **C**) were sacrificed at the endpoint of experiments in Figure 2G, Figure 2H and Figure 3A, respectively. TDLN cells were analyzed by FACS for DC populations. DCs were gated on CD11c$^+$ cells, and the total number of CD8α$^+$ DCs and CD11b$^+$ DCs were calculated from TDLNs (n = 3~4/group). The *p* values in the graphs show comparison with PBS or as indicated.

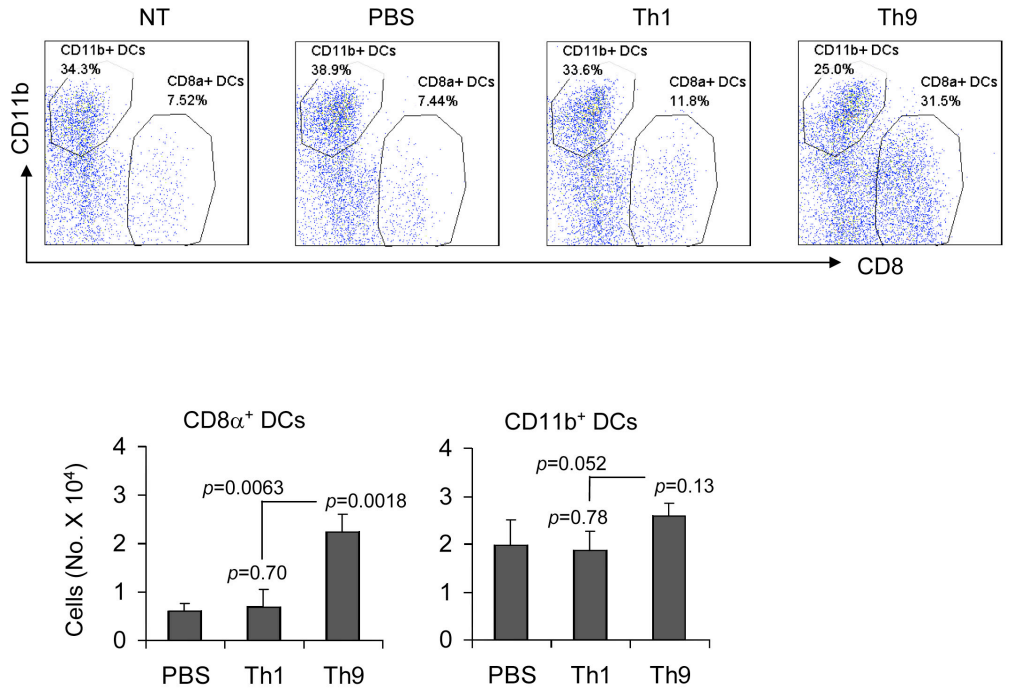

Supplementary Figure 10

Supplementary Figure 10. Infiltration of CD11c$^+$ DCs in the lung. PBS or 3 × 10^6 Th1 or Th9 cells were i.v. transferred into C57BL/6 mice bearing 5-day established pulmonary B16-OVA melanoma. Mice were sacrificed 4 days later, and lung cells were analyzed by FACS for DC populations. DCs were gated on CD11c$^+$ cells, and the frequency of DCs subsets in CD11c$^+$ cells was shown (upper panels). Lower panels show the total number of CD8α$^+$ DCs and CD11b$^+$ DCs in the lung leukocyte fraction calculated from mice (n = 3~4/group). The *p* values in the graphs show comparison with PBS or as indicated.

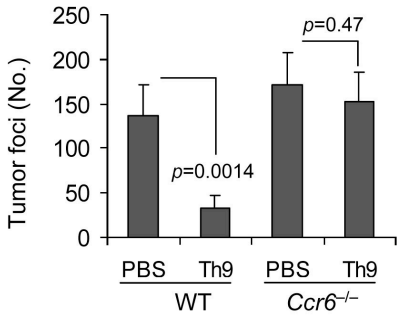

Supplementary Figure 11

Supplementary Figure 11. Tumor foci numbers of treated mice. PBS or 3×10^6 Th9 cells were transferred to mice (wild-type and *Ccr6*$^{-/-}$ mice; n =4/group) bearing 5-day established pulmonary B16-OVA melanoma. Shown are the lung foci numbers observed on day 19 after challenge.

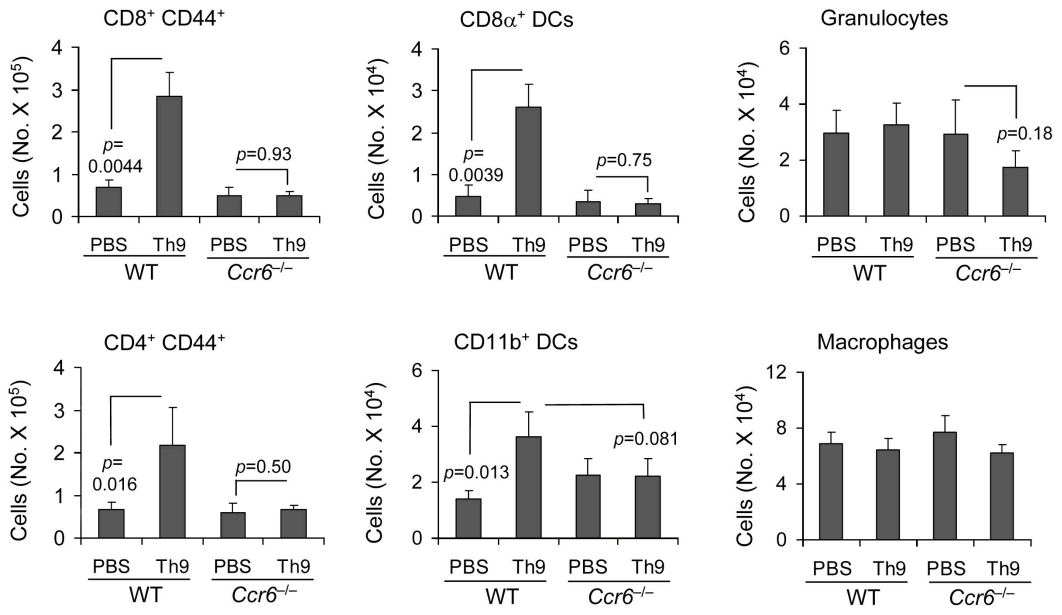

Supplementary Figure 12

Supplementary Figure 12. Infiltration of leucocytes in the lung. PBS or 3×10^6 Th9 cells were i.v. transferred into mice (n = 4/group; wild-type and *Ccr6*$^{-/-}$ mice) bearing 5-day established pulmonary B16-OVA melanoma. Mice were sacrificed on day 19 after challenge. Lung leukocytes were analyzed by FACS. Total numbers of indicated subsets are calculated. The *p* values are shown as indicated.